A Novel Inductor Loss Calculation Method on Power Converters Based on Dynamic Minor Loop

Seiji Iyasu Student Member (Tokyo Metropolitan University, iyasu@pe.eei.metro-u.ac.jp)
Toshihisa Shimizu Senior Member (Tokyo Metropolitan University, shimizu@eei.metro-u.ac.jp)
Kenichiro Ishii Member (TOHO ZINC Co., Ltd., hanako@denki.ac.jp)

Keywords: dynamic minor loop, iron loss, loss map, and PWM inverter

In order to increase both the conversion efficiency and the power density of the power converters, a study on the loss reduction method on the magnetic component is one of the most important issue among the power electronics authorities. Traditionally, reduction methods of the magnetizing loss on the transformers and the ac motors have been studied. However, not so many reports regarding the inductor iron loss on the ac/dc filter inductor under the use of the high-frequency PWM switching condition have been reported. Difference of the iron loss between the transformers and the inductors depends deeply on both the amplitude and the waveform of the magnetizing current flowing thorough them. Especially on the inductors, the low-frequency current depends on the output current, and the high-frequency ripple current depends on the modulation condition of the converters. This means that the magnetic operating point and the shape of dynamic minor loop are changed according to the instantaneous amplitude of the low-frequency current. Also, the sum of the loss caused by dynamic minor loop usually dominate the iron loss of the inductor. Hence the loss calculation on the inductors are usually complicated compared to that on the transformers.

Fig. 1 shows the proposed measuring system for the iron loss. This measuring system enables to measure the accurate iron loss. Also, this paper proposes a novel loss-map of the magnetic materials as shown in Fig. 2. By using this loss map, we can calculate the iron loss on the inductors in many kinds of converters by taking the magnetizing conditions of the inductors into account. In the case when we calculate the iron loss on the inductor on DC-DC converter, it is enough to multiply the data on the loss map the switching frequency and the volume of the core. Futhermore, we propose a novel iron loss calculation method of the ac filter inductor on the PWM inverter by using the loss map. It is verified that the calculated results of the iron loss of the AC filter inductor on the PWM inverter coincide well the those on the experimental set up. It is concluded that the proposed loss map and the iron loss calculation method is useful for designing the optimal inductor used on the switching converters.

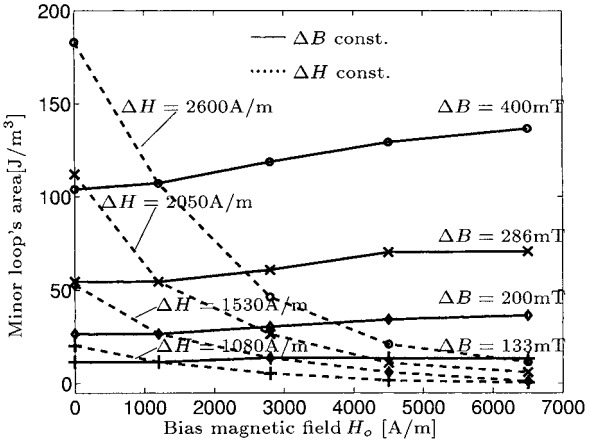

Fig. 2. Loss map of the magnetic material (SK-core)

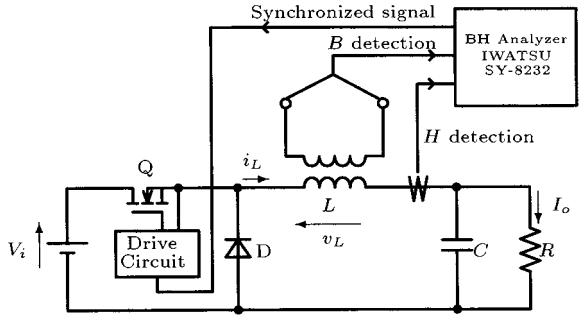

Fig. 1. Mesuring system

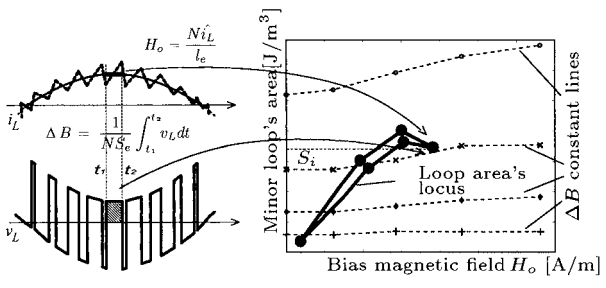

Fig. 3. Iron loss calculation method on PWM inverters

Paper

A Novel Inductor Loss Calculation Method on Power Converters Based on Dynamic Minor Loop

Seiji Iyasu* Student Member
Toshihisa Shimizu* Senior Member
Kenichiro Ishii** Member

This paper proposes a novel iron loss calculation method based on the loss-map of the magnetic materials. The distinctive feature of this method is that the iron loss on the inductors in many kinds of converters can easily be calculated even if the magnetizing conditions of the inductors are different. In this paper, the dynamic minor loop characteristics of the magnetic core on the condition of the switching converter are defined. Then, the dynamic measuring method of the dynamic minor loop by using the chopper circuit is presented. Next, some typical loss characteristics derived from the dynamic minor loop measurement is discussed. Also, a novel loss calculation method of the ac filter inductor on the PWM inverter by using the modified loss-map method is proposed.

Keywords: dynamic minor loop, iron loss, loss map and PWM inverter

1. Introduction

In recent years, remarkable loss reduction of the power semiconductors have been achieved, and as a result, the loss of the magnetic components, such as the transformers and the inductors, used in the power converters becomes relatively increasing. In order to increase both the conversion efficiency and the power density of the power converters, a study on the loss reduction method on the magnetic component is one of the most important issue among the power electronics authorities. Traditionally, reduction methods of the magnetizing loss of the transformers and the ac motors have been studied [(1)–(4)]. However, only a few papers have been reported the inductor iron loss of the ac/dc filter inductor under the use of the high-frequency PWM switching condition. In this case, the magnetic trajectory on the BH-plane has two kind of the magnetic loops. The one is caused by the low-frequency current which depends on the output current and another is caused by the high-frequency ripple current which depends on the modulation condition of the inverter [(7)]. In this paper, the former magnetic loop is called a major loop and the later magnetic loop is called a dynamic minor loop. Also, it is well known that the magnetic operating point and the shape of dynamic minor loop are changed according to the instantaneous amplitude of the low-frequency current. Especially, in the case when the switching frequency is much higher than the output frequency, the loss caused by dynamic minor loops (the high-frequency ripple current) usually dominate the iron loss of the inductor. Hence the loss calculation on the inductors are usually complicated compared to that on the transformers. However it is difficult to calculate the iron loss caused by the high-frequency ripple current on the above condition because the magnetic component suppliers provide only a few loss data taking those high frequency ripple current into account. P. Tenant et al. have reported a prediction method of the iron loss of the inductor used in the DC-DC converters based on dynamic minor loop [(5)]. In this method, the iron loss is calculated on the basis of numerical dynamic minor loop which takes hysteresis loss, eddy current loss, and residual loss into account. However, some experimental data are necessary in order to adjust the numerical parameter in the numerical equation. Then, it is difficult to apply this method in designing the inductor used in many kinds of converters with the different conditions.

This paper proposes a novel iron loss calculation method based on the loss-map of the magnetic materials. Once the loss-map is generated from the measured result, it can easily be applicable to many kinds of converters even if the magnetizing conditions of the inductors are different. In this paper, the dynamic minor loop characteristics of the magnetic core in the use of the switching converter are defined. Then, the dynamic measuring method of the dynamic minor loop by using the buck-chopper circuit is presented. Next, some typical loss characteristics derived from the dynamic minor loop measurement is discussed. Also, a novel loss calculation method of the ac filter inductor in the PWM inverter by using the loss map method is proposed. The calculated losses are verified through the experiments. Finally, our future works for the loss map method are also mentioned.

2. Dynamic Minor Loop of the Inductor

Firstly, we briefly review the dynamic minor loop and the resultant iron loss under the condition of rectangular voltage excitation. Figs. 1(a) and (b) show the buck chopper circuit and its operating waveforms. The waveforms of both the magnetic field, H, and the flux density, B, strongly depend on the current which contains the ripple component and the dc-bias component, and the operating frequency. The amplitude of the magnetic field ripple, ΔH, the amplitude of the

* Depatrment of Electrical Engineering, Tokyo Metropolitan University 1-1, Minami-osawa, Hachioji 192-0397, JAPAN
** TOHO ZINC Co., Ltd, Naka 387, Fujiokashi, Gunma 375-0005, JAPAN

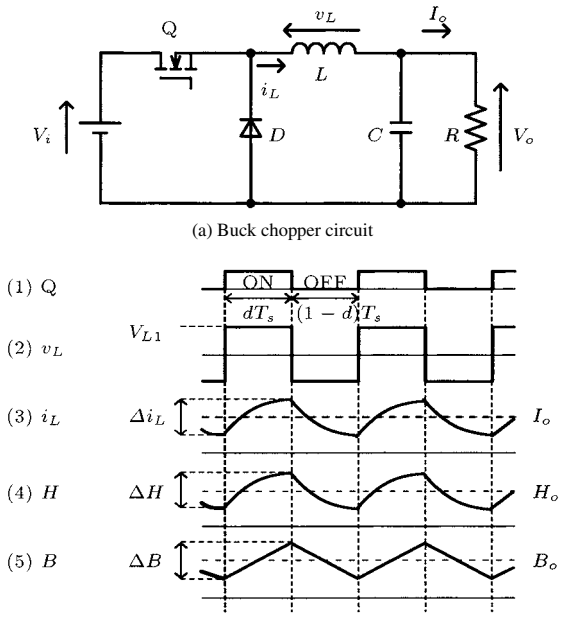

(a) Buck chopper circuit

(b) Operating waveforms on the chopper circuit

Fig. 1. The buck chopper circuit and its operation waveforms

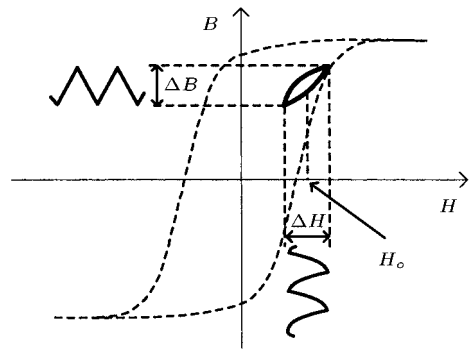

(a) Dynamic minor loop under the rectangular voltage excitation (on the buck-chopper)

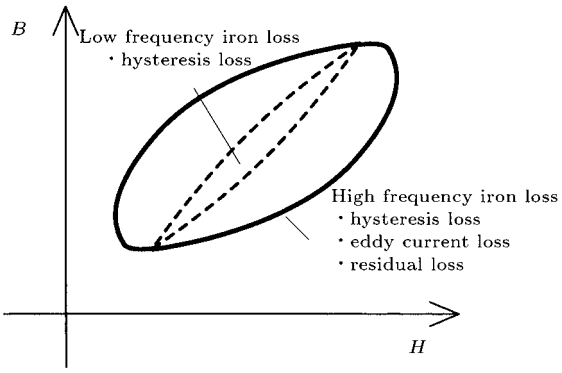

(b) Dynamic minor loop and iron loss

Fig. 2. Dynamic minor loop

flux density ripple, ΔB, and the dc-bias magnetic field, H_o are calculated from the following equations.

$$\Delta B = \frac{\Delta\phi}{S_e} = \frac{1}{NS_e}\int_0^{dT_s} v_L dt = \frac{V_{L1}d}{Nf_sS_e} \cdots\cdots\cdots (1)$$

$$\Delta H = \frac{N\Delta i_L}{l_e} = \frac{V_{L1}dN}{Lf_sl_e} = \frac{V_{L1}d}{\mu Nf_sS_e} \cdots\cdots\cdots (2)$$

$$H_o = \frac{NI_o}{l_e} = \frac{NdV_i}{Rl_e} \cdots\cdots\cdots (3)$$

Where, N, l_e and S_e are the turn number of the windings of the inductor, the effective magnetic length and the effective cross sectional area of the magnetic core, respectively.

Because of the time delay of magnetization, the waveform of magnetic field, H, becomes distorted from triangular-wave as shown in Fig. 1(b). Therefore the dynamic minor loop on the BH-plane can be illustrated as shown in Fig. 2(a). The iron loss on the inductor corresponds to the area surrounded by this loop. The area sometimes becomes large, as shown in Fig. 2(b), due to the increase of the eddy current loss and the residual loss at very high frequency switching condition.

Above mentioned loss caused by the dynamic minor loop deeply depends on the induced voltage/current waveforms, the dc-bias condition and the switching frequency as well as the magnetic hysteresis characteristics [7]. However, traditional loss characteristic data supplied from the magnetic material suppliers are usually the one measured on the sinusoidal voltage excitation with no dc bias. Hence, the expected loss calculated from those data sheets usually differs from the actual one. Then, most of the power electronics designers usually have to measure the inductor loss on the experimental setup at their laboratory. A novel loss calculation method based on the dynamic loss measurement presented in this paper can remove this exhaustive work and make the converter design efficient. In the first step, the measuring method of the dynamic minor loop is proposed, and the iron loss characteristics obtained from this method is discussed. In the next step, the novel loss map which reflects the iron loss characteristics is created. Finally, the loss calculation method of ac filter inductor used in the PWM inverter are proposed.

3. Measuring System

Fig. 3 shows the measuring system for the dynamic minor loop of the inductor under the rectangular voltage excitation. In order to induce the rectangular voltage to the inductors, a buck chopper circuit is used. Table 1 shows the specification of the inductor used under the test. The core material of this inductor is the iron powder compressed core. In order to avoid the influence of air gap, a toroidal core was used. The flux density, B, is detected by the secondary winding in order to avoid the influence of the voltage drop of the winding resistance. Also, the secondary winding is carefully wound so as not to create the parasitic capacitor between the winding.

In order to measure the iron loss accurately, it is essential to detect the accurate magnetic field, H. In this measuring system, the magnetic field is detected by Tektronix A6303 dc current probe. V.J. Thottuvelil et al. have reported the current probe is inappropriate for the accurate magnetic field detection due to its large error phase angle between the actual current and the detected signal on the current probe [6]. Fig. 4 shows the measured percent error of the iron loss. Horizontal axis shows the real phase angle, θ, between the inductor voltage and the inductor current, and the vertical axis shows the percent error of the iron loss when the error angle, α, is contained in the current measuring signal. The percent error

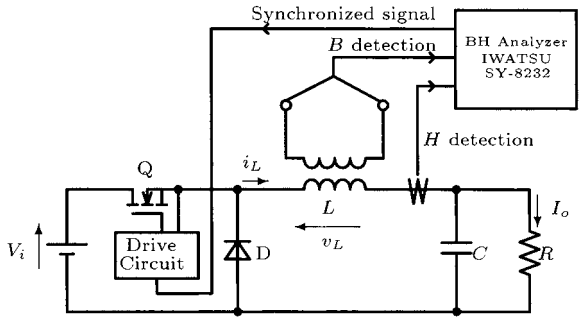

Fig. 3. Mesuring system

Table 1. Specification of Inductor (SK-14M (TOHO ZINC Co., LTD))

Core Material	Iron Powder Compressed Core
Shape	Toroidal
Effective Magnetic Path Length, l_e	61.24 mm
Effective Cross Sectional Area, S_e	74.19 mm^2
Volume, V_e	4543 mm^3
Weight, M	32 g
Turn, N	50 turn
Inductance, L	266 μH

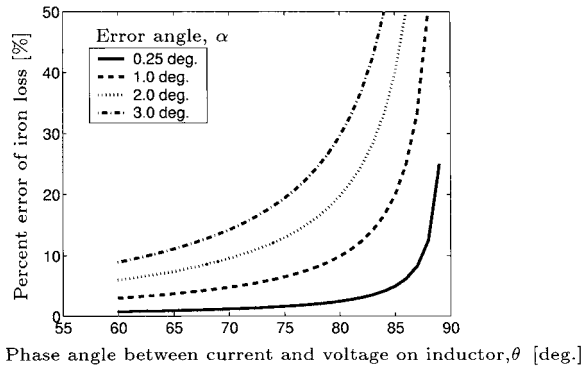

Fig. 4. Percent error of iron loss vs. phase angle between inductor current and inductor voltage

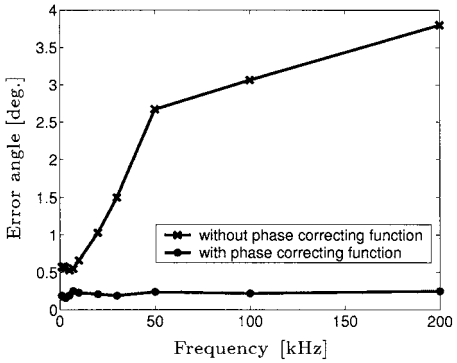

Fig. 5. Error angle vs. frequency characteristics on A6303 (Tektronix)

is defined as following equations.

$$\text{percent error} = \frac{\text{(real iron loss)}}{\text{(real iron loss) + (measuring error)}} \times 100 \cdots\cdots (4)$$

$$= \frac{[\cos(\theta-\alpha) - \cos\theta]}{\cos\theta} \times 100 \cdots\cdots\cdots\cdots\cdots (5)$$

It can be seen that the lower the error angle takes, the lower the percent error becomes. On the ideal inductor, the phase angle, θ, takes 90 deg. However, the value of the phase angle, θ, decreases on the practical inductor because of the iron loss. It is also obvious that the percent error is critically affected by the error angle, α, when the phase angle, θ, is larger. This means that we should decrease the error angle, α, as small as possible. In our study, we used the material as SK-14M which takes the value of the phase angle, θ, around 80 to 86 deg. We decreased the error angle, α, to 0.25 deg by using the dynamic phase correcting function on the B-H analyzer as shown in Fig. 5. Hence the percent error of the iron loss on this study can be reduced to less than 5%.

The chopper circuit is operated synchronized with the pulse signal, in this case 10000 pulse, that is generated by the BH analyzer. The trajectories on the B-H plane for each pulse are converged to an averaged loop, and hence the measurement error, which is caused by the temperature rise of the winding and the electrical noise, can be mitigated. As a result, the accurate iron loss caused by the dynamic minor loop can be measured by this system.

4. Measured Results and Loss Map of the Magnetic Materials

4.1 Influence of Bias Magnetic Field In the measuring system shown in Fig. 3, the input voltage and the duty ratio of the switch, Q, are set to 30 V and 50%, respectively. By changing the output current, I_o, from 1.5 A to 8 A, the bias magnetic field, H_o, is changed from 1230 A/m to 6500 A/m. The iron losses are measured under two conditions, such that ΔB is kept constant or ΔH is kept constant regardless of change of H_o. The "constant ΔB" condition corresponds to the operation under the voltage pulse width modulation, and the "constant ΔH" condition corresponds to the operation under the current hysteresis modulation. Fig. 6 shows the measured results of the dynamic minor loop under above conditions as the bias magnetic field, H_o, is changed from 1230 A/m to 6500 A/m. Figs. 6(a) and (b) show that the value of ΔH and the area surrounded by the dynamic minor loop increases as the bias magnetic field, H_o, increases under the "constant ΔB" condition. This is because that the inductance, L, reduces as the bias magnetic field, H_o, increases. This fact shows the iron loss increases as the bias magnetic field, H_o, increases under the "constant ΔB" condition. Figs. 6(a) and (c) show that the value of ΔB and the area surrounded by the dynamic minor loop decreases even though bias magnetic field, H_o, increases under the "constant ΔH" condition. This is because that the shape of the loop comes to narrow as bias magnetic field, H_o, increases.

4.2 Frequency Dependency Here we discuss the frequency dependency of the iron loss on SK-14M. The frequency is changed from 5 kHz to 20 kHz. Figs. 7(a) and (b) show the dynamic minor loops at the frequency of 5 kHz and 10 kHz, respectively. ΔB and H_o are adjusted to 400 mT and 1230 A/m, respectively. Figs. 8(a) and (b) show the frequency dependency of the iron loss and that of the dynamic minor loop, respectively. We can see that the shape of minor loop and the resultant minor loop's area of this material do not changed in this frequency band. It is predicted that the hysteresis loss on this material is dominant in the iron loss in this frequency band, such as from 5 kHz to 20 kHz. It should be

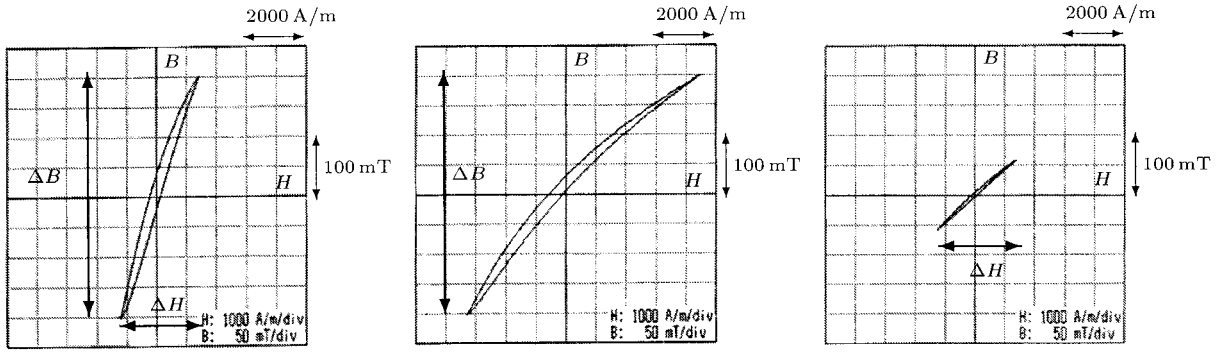

(a) ΔB = 400 mT, ΔH = 2600 A/m, H_o = 1230 A/m

(b) The "constant ΔB" condition (ΔB = 400 mT, H_o = 6500 A/m)

(c) The "constant ΔH" condition (ΔH = 2600 A/m, H_o = 6500 A/m)

Fig. 6. Dynamic magnetic minor magnetic loops when ΔH kept constant and ΔB kept constant

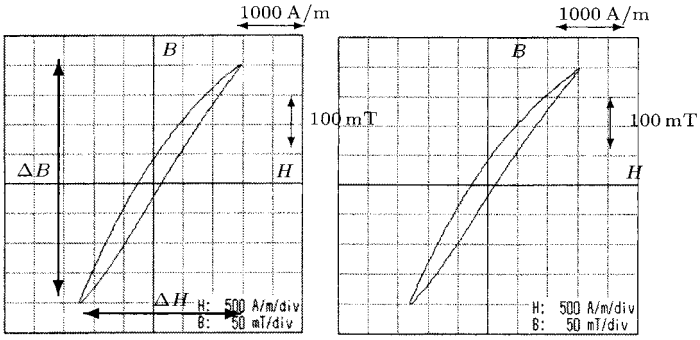

(a) f_s = 5 kHz (b) f_s = 10 kHz

Fig. 7. Frequency dependency of minor loop under same ΔB, H_o (ΔB = 400 mT, H_o = 1230 A/m)

noted that the shape of dynamic minor loop may vary in the case when the switching frequency is much higher than that we measured. Because the eddy current loss may increase. However, in this study, we can neglected those effects by setting the switching frequency to 15 kHz in order to clarify the basic concept of the proposed method.

4.3 Loss Map of Magnetic Materials Figs. 9 shows the novel loss map obtained from above mentioned experimental results. This loss map is expressed by bias magnetic field, H_o, and area of dynamic minor loop [J/m^3] with parameters of ΔH and ΔB. This loss map does not depend on the core size and turn number of the winding, since BH-curve characteristics usually depend on the core material. Then this loss map enables to predict the iron loss of the inductors under arbitrary conditions. In the case when we calculate the iron loss of the filter inductor on the DC-DC converters, the iron loss can be calculated very easily. Substituting some operation parameters on the inductor in the equation (1) and (3), then we read out the value of the minor loop's area on the loss map. Hence, we can evaluate the iron loss by multiplying the area of this loss map by switching frequency and the volume of the core. At very high frequency conditions, as the eddy current loss and the residual loss can not be negligible, the actual area surrounded by the dynamic minor loop will increase from the area shown in this loss map. In this case, it is enough to multiply the value on the loss map by some coefficient. Derivation of the coefficients will be the future work in our group.

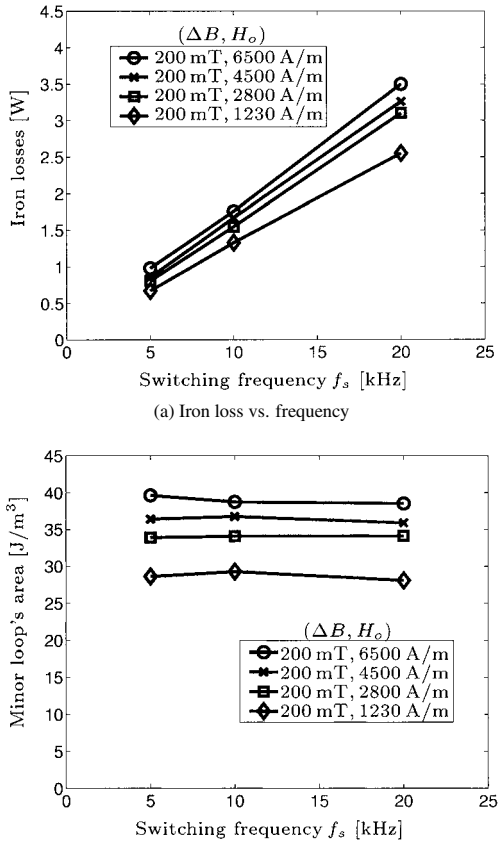

(a) Iron loss vs. frequency

(b) Minor loop's area vs. frequency

Fig. 8. Frequency dependency of the iron loss on SK-14M

5. A Novel Calculation Method of AC Filter Inductors on Voltage Source PWM Inverters

5.1 Dynamic Minor Loops of AC Inductors on PWM Inverters Fig. 10 shows a single phase PWM inverter including an AC filter circuit. Fig. 11(a) shows the operation waveforms and Fig. 11(b) shows a part of the dynamic minor loop of the AC inductor core which correspond to the waveforms surrounded by the circles in Fig. 11(a). As shown in Fig. 11(a), bias magnetic field changes dynamically due to the change of output current. Then, the dynamic minor loop of the AC inductor core in one switching period becomes to

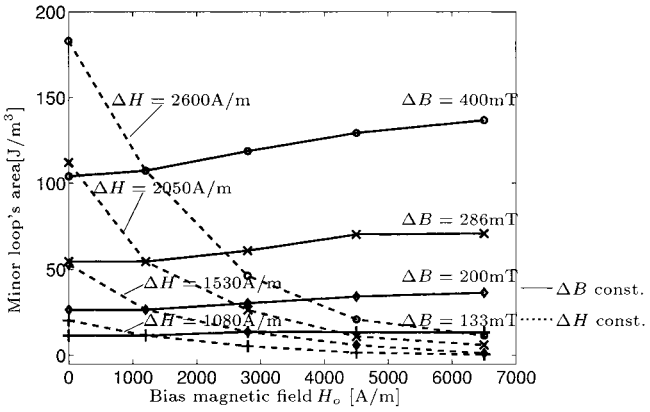

Fig. 9. Loss map of the magnetic material (SK-core)

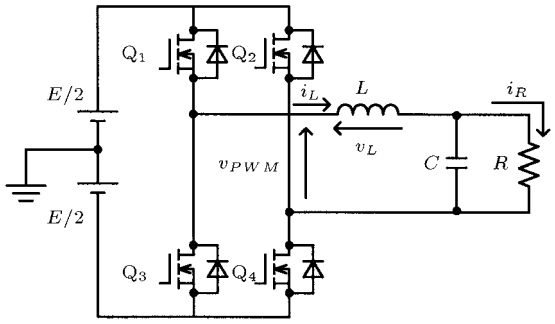

Fig. 10. Single phase PWM inverter

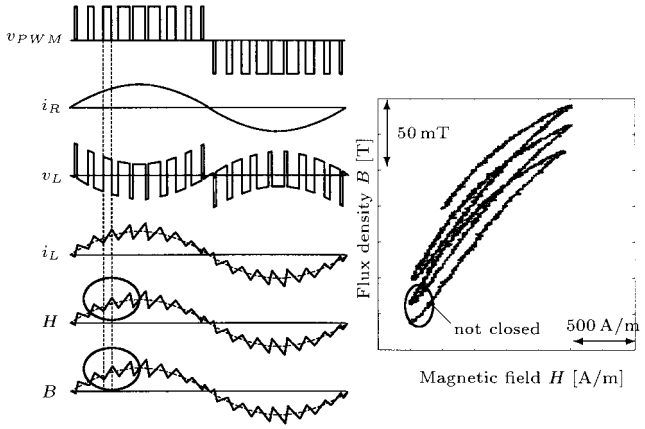

(a) Operation waveforms (b) Dynamic loop

Fig. 11. Operation waveforms and dynamic loop on PWM inverter

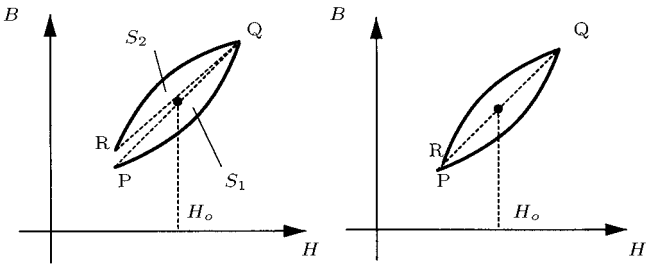

(a) Dynamic minor loop on PWM inverter at one switching period (b) Quasi-closed loop

Fig. 12. Approximation to the quasi-closed loop

open-loop shape, as shown in Fig. 11(b). It seems to be difficult to predict the iron loss because the trajectory does not form closed-loop at each switching interval.

5.2 Approximation Method of the Dynamic Minor Loops In order to make the iron loss calculation possible, this paper presents an approximation method of the dynamic minor loop of ac filter inductor. Fig. 12(a) shows the magnetic trajectory(dynamic minor loop) on the B-H plane during one switching period. The magnetic operating point on the trajectory moves from P to Q and ends at R. Then we also can assume that the sum of the area, S_1, surrounded by the arc $\widehat{\mathrm{PQ}}$ and the line $\overline{\mathrm{PQ}}$, and the area, S_2, surrounded by the arc $\widehat{\mathrm{QR}}$ and the line $\overline{\mathrm{QR}}$ corresponds to the iron loss during one switching period. If we assume that the iron loss caused by the high-frequency ripple current is negligible, the trajectory on the B-H plane of the magnetic material may trace on the lines $\overline{\mathrm{PQ}}$ and $\overline{\mathrm{QR}}$. In the case when the switching frequency of the PWM inverter is much higher than its output frequency, the starting point P of the trajectory is very close to the ending point R. Here, when we move the arc $\widehat{\mathrm{QR}}$ so that the line $\overline{\mathrm{QR}}$ is superimposes to the line $\overline{\mathrm{PQ}}$ as shown in the Fig. 12(b), the area surrounded by the figure PQRP coincide with the sum of S_1 and S_2. In this study, we call this figure as the quasi-closed loop. And the shape of this quasi-closed loop is also similar to the dynamic minor loop on the buck-chopper circuit in the previous section. Fig. 13(b) shows the measured result of the dynamic minor loop of the inductor on the PWM inverter. Table 2 shows the circuit parameters of the PWM inverter. Fig. 13(a) shows the measured dynamic minor loop of the inductor on the buck chopper circuit. The magnetizing condition of the dynamic minor loop is set to ΔB = 235 mT and H_o = 2000 A/m in both converters. The area of the dynamic minor loop calculated from Fig. 13(a), which is same with the one obtained from the loss map shown in Fig. 9, is 41.6 J/m^3. On the other hand, the area of equivalent quasi-closed loop calculated from Fig. 13(b) is 41.4 J/m^3. It is clear that those values coincide well.

Fig. 14 shows the experimental results of the inductor current, i_L, the low-frequency current component of the inductor current, $\bar{i_L}$, the flux density ripple, ΔB, and the corresponding areas of the quasi-closed loops, S. The areas obtained from the loss map under same condition of ΔB and H_o with the PWM inverter, are also shown in Fig. 14. The areas of the quasi-closed loop of the AC filter inductor on PWM inverter coincide well with those obtained from the loss map. This result clearly shows that the proposed approximation method is appropriate for iron loss calculation.

5.3 Inductor Iron Loss Calculation Method on PWM Inverters Usually, both the low-frequency current component of the inductor current and the variation of the value of ΔB on the ideal inductor are almost same with those on the practical inductor. Then the variation of value of ΔB and H_o in each switching interval can be calculated by using adequate circuit simulation software such as P-spice and P-SIM. By using this result, the dynamic loop's areas of the inductor, S_i, in each switching period can be plotted , of those are denoted by "•", in the loss map as shown in Fig. 15. Loop area's locus can be drawn by tracing each point, and the shape of the locus expresses the loss distribution corresponding to both the output current waveform and the modulating condition. Once we can get this loss distribution, the iron loss of

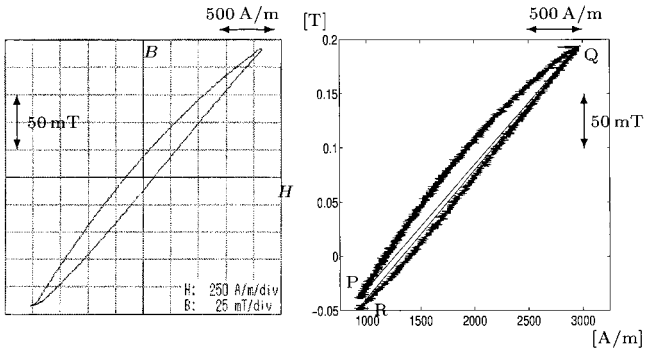

(a) Under the buck chopper circuit (b) Under the PWM inverter

Fig. 13. Dynamic minor loops when ΔB = 235 mT, H_o = 2000 A/m

Table 2. Circuit parameters for experiment

Input Voltage, E	60 V
Output Filter Inductance, L (Table 1)	266 μH
Output Filter Capacitance, C	50 μF
Output Resistance, R	10 Ω
Output Frequency, f_o	50 Hz
Switching Frequency, f_s	15 kHz
Modulation Index	0.83

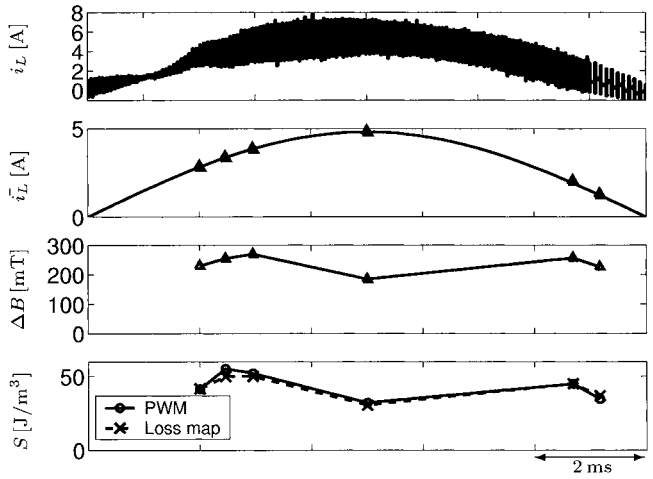

Fig. 14. Experimental results and the areas obtained from the loss map

the filter inductor can be calculated from the following equation.

$$P = 2 \cdot V_e \cdot f_o \cdot \sum_{i=1}^{n} S_i \quad \cdots\cdots\cdots\cdots\cdots\cdots\cdots\cdots (6)$$

Where, V_e is the volume of the inductor core, f_o is the output frequency which is same with the low-frequency current of the inductor, S_i is the area surrounded by the quasi-closed loop in each switching period, n is the number of the quasi-closed loop in half cycle of the low-frequency current.

5.4 Verification of Inductor Iron Loss Calculation Method on PWM Inverters The proposed iron loss calculation can be executed by P-SIM. Table 2 shows the circuit parameters on the simulation. Fig. 16(a) shows the simulation result of the inductor current, i_L, the inductor voltage, v_L, the bias magnetic field, H_o, the flux density ripple, ΔB, and Fig. 16(b) shows the area's locus on the loss map. Table 3 shows the iron loss obtained from both the calculation

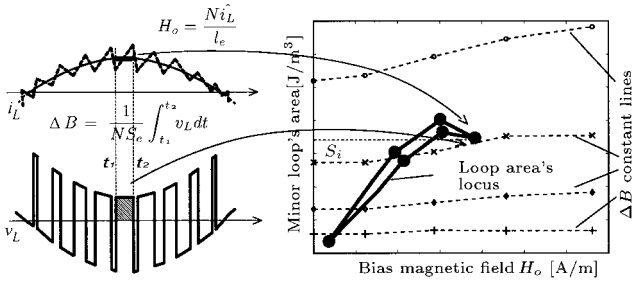

Fig. 15. Iron loss calculation method on PWM inverters

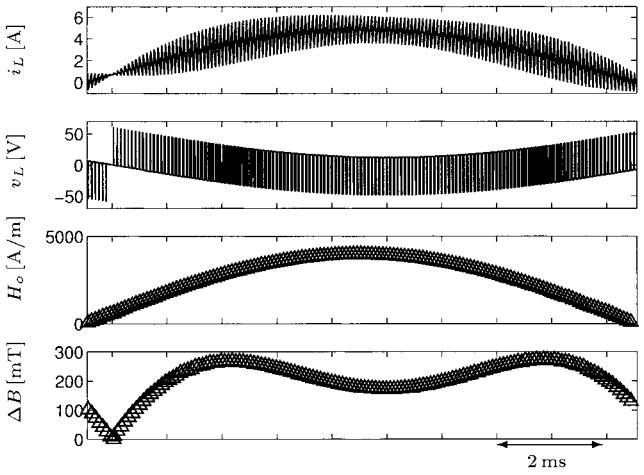

(a) Simulation waveforms for iron loss calculation

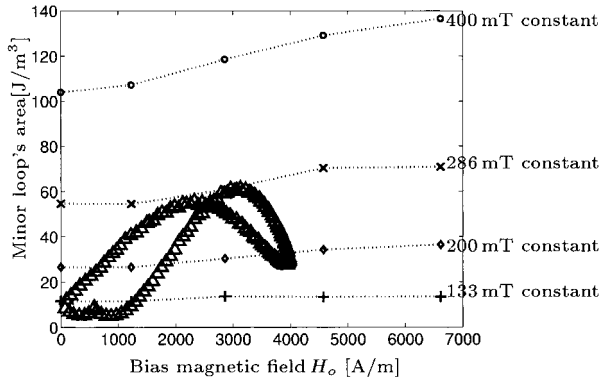

(b) The area's locus on the loss map

Fig. 16. Iron loss calculation result obtained by using P-SIM

Table 3. Experimental result and calculation result

	Experimental result	Calculation result
Iron Loss [W]	2.93	2.62

method and the experimental setup. In order to measure the iron loss, the power-analyzer PZ4000(YOKOGAWA) was used. Taking the error of the power analyzer and the error of the loss map into account, it can be concluded that the calculated loss coincide well with the measured one. Hence, it is verified that the proposed iron loss calculation method of the ac filter inductor on the PWM inverter is useful.

6. Conclusions

The authors discussed a measuring method of dynamic minor loop and the resultant iron loss, and presented a novel loss map of magnetic materials on the basis of the dynamic

minor loop. The loss map enables to predict the iron loss of the inductor on the DC-DC converters. Furthermore, a calculation method of the iron loss of the ac filter inductor on the PWM inverter is also proposed. It is verified that the calculated results of the iron loss of the AC filter inductor on the PWM inverter coincide well with those on the experimental set up. It is concluded that the proposed loss map and the iron loss calculation method is useful for designing the optimal inductor used on the switching converters. Based on the proposed loss map, development of the optimal modulation method that reduces the inductor loss on the inverter is the future work.

(Manuscript received May 26, 2005,
revised Jan. 24, 2006)

References

(1) A. Boglietti, P. Ferraris, M. Lazzari, and F. Profumo: "Effects of Different Modulation Index on the Iron Losses in Soft Magnetic Materials Suppulied by PWM Inverter", *IEEE Trans. Magnetics*, Vol.29, No.6, pp.3234–3236 (1993)

(2) A.J. Moses and N. Tutkun: "Investigation of Power Loss in Wound Toroidal Cores under PWM Excitation", *IEEE Trans. Magnetics*, Vol.33, No.5, pp.3763–3765 (1997)

(3) A. Boglietti, P. Ferraris, M. Lazzari, and M. Pastorelli: "Influence of Modulation Techniques on Iron Losses with Single Phase DC/AC Converters", *IEEE Trans. Magnetics*, Vol.32, No.5, pp.4884–4886 (1996)

(4) A. Boglietti, P. Ferraris, M. Lazzari, and M. Pastorelli: "About the Possibility of Defining a Standard Method for Iron Loss Measurement in Soft Magnetic Materials with Inverter Supply", *IEEE Trans. IA*, Vol.33, No.5, pp.1283–1288 (1997)

(5) P. Tenant and J.J. Rousseau: "Dynamic Model of Magnetic Materials Applied on Soft Ferrites", *IEEE Trans. Power Electron.*, Vol.13, pp.372–379 (1998)

(6) V.J. Thottuvelil, T.G. Wilson, and H.A. Owen: "High Frequency Measurement Techniques for Magnetic Cores", *IEEE Trans. Power Electron.*, Vol.5, pp.41–53 (1990)

(7) T. Shimizu, K. mishima, K. Wada, and K. Ishii: "Mitigation of Inductor Loss Based on Minor-Loop Hysteresis Characteristics", IEICE/IEEE INTELEC, pp.834–839 (2003)

Seiji Iyasu (Student Member) was born in Hiroshima, Japan, in 1981.

He received the B.S. and M.S. degrees both in electrical engineering from Tokyo Metropolitan University, Hachioji, Japan, in 2004 and 2006, respectively. In 2006, he joined Denso Ltd., Kariya City, Japan. His research interests include power electronics circuits and AC filter inductor.

Toshihisa Shimizu (Senior Member) was born in Tokyo, Japan, in 1955.

He received the B.S., M.S. and Dr.Eng. degrees all in electrical engineering from Tokyo Metropolitan University, Hachioji, Japan, in 1978, 1980 and 1991, respectively. In 1998, he was a Visiting Professor at Virginia Polytechnic Institute and State University, Blacksburg, the United States. He joined Fuji Electric Corporate Research and Development, Ltd. in 1980. In 1993, he joined the Department of Electrical Engineering, Tokyo Metropolitan University, as an Associate Professor. Since 2005, he has been a Full Professor. His research interests include power converters, high frequency inverters, photovoltaic power generations, UPS's, EMI problems, AC filters and High-power density converters, etc. Dr.Shimizu received the Transaction Paper Award from the Institute of Electrical Engineers of Japan in 1999. He is a senior member of the Institute of Electrical and Electronics Engineers.

Kenichiro Ishii (Member) was born in Tokyo, Japan, in 1967.

He received the B.S. degree in electrical engineering from Nihon University, Tokyo, Japan, in 1990. In 1990, he joined Toho Zinc Ltd., Fujioka City, Japan. His research interests include EMI filter and inductors.